Gazi University

Journal of Science

http://dergipark.gov.tr/gujs

Differential Depletion Charge Density of the Approximation of Schottky Diodes as Ohmic Annealed a Variety of Temperatures

Abdulkadir Korkut[*]

Yuzuncu Yil University Science Faculty, Department of Physics, Tusba, 65080, Van Turkey

Highlights
• The differential depletion charge density formulae are find out for both forward and reverse bias.
• Values on zero-voltage differential depletion charge density rise by increasing ohmic temperature.
• The expanded series fitting equations obey to the rule of m_1-m_2=0 in analytic geometry.

Article Info

Abstract

This study aimed to investigate the differential depletion charge density for (Ag, Cu, Ni) /n-Si/Al Schottky diodes which depend on ohmic contact temperatures. Ohmic contact temperature defines the Schottky diode parameters. Furthermore, ohmic temperature is concerned with diode quality. In general, depletion charge density is determined as depending on built-in potential. The differential depletion charge density is smaller than zero-voltage depletion charge density (V = 0, Vbi ≠ 0) in the case of forward bias and higher than the zero-voltage depletion charge density for reverse bias. When the depletion charge density formula was expanded into a series, new equations revealed appreciable results. Boundary-values were found for differential depletion charge density using normal and expanded formulae.

1. INTRODUCTION

It is well known that the metal-semiconductor (MS) interface is very important for the electrical characteristics of Schottky diodes. If the pure metal, which should be noted that differential work function for *n*-type, is evaporated the ohmic side and the Schottky side of the semiconductor surface, all parameters belonging to the Schottky diodes will change. In this article, Schottky parameters have been examined for both situations; forward bias and reverse bias. Ideality factor (IF) (n_{IV}) [1, 2], barrier height (Φ_{BH}) [3, 4], Cheung functions (Ch1, Ch2) [5, 6], built-in potential (V_{bi}) [1, 2], donor density (N_D) [7], zero-voltage depletion length (W_0 or L_0), interfacial thickness (D_{it}) [6], interface state density (N_{SS}) [8, 9] and effective Fermi level (E_F) are known as Schottky parameters [10]. A Schottky diode is comprised of four sections, namely ohmic junction, base structure, depletion layer and Schottky junction [10, 11]. The depletion layer (or length) is the most important part of a Schottky diode. The depletion layer length, which is a solution of Poisson equation, is a parameter of the dimension of length [7, 10]. Most of the physical parameters such as depletion layer length [12], depletion capacitance change and depletion charge density (DCD) vary in the depletion layer [13-15]. The depletion capacitance changes with depletion layer length and the DCD varies with depletion layer length [11-14, 15]. The mentioned parameters of a Schottky diode are used to obtain the characteristics of the diode. This study aimed to understand the characteristic changes of Schottky MS diodes in the DCD and differential depletion charge density (DDCD) [11, 14]. (Ag, Cu, Ni)/*n*-Si/Al Schottky diodes were fabricated and analyzed to detect the characteristic changes in the DCD and DDCD according to the increasing ohmic temperatures. Selecting ohmic temperature is a very important process as selecting the wrong temperature directly affects the Schottky diode parameters, one of which is DCD.

*e-mail: akkut@yyu.edu.tr

2. MATERIAL AND METHODS

2.1. Diode Fabrication

In the fabrication process of making the diode, *n*-Si wafers, 450 μm in thicknesses and with ρ=1-10 Ω.cm resistivity and (100) orientation were used. The n-Si wafer was chemically cleaned of chemical and organic contaminants [1, 2, 7]. The n-Si wafer was then boiled for 3 min. in a ($NH_4H+H_2O_2+6H_2O$) solution and 3 min. in a ($HCl+H_2O_2+6H_2O$) solution using RCA, which is a method developed by W. Kern in the Radio Corporation of America [16]. The n-Si wafer was etched in $HF:H_2O$ (1:10) for 30 s. and rinsed with deionized water with ultrasonic vibration. The n-Si wafer was cut into 20 pieces as the surface area consisted of 25 mm². Next, the reverse sides of the pieces formed ohmic contact by evaporating cleaned Al at the 10^{-6} Torr pressure in the vacuum. They annealed 400^0C, 420^0C, 440^0C, 460^0C, 480^0C for 3 min in flowing N_2 gas. Thus, ohmic contact was formed for all samples. One of the samples was instantly inserted into the evaporation chamber (model: Edwards A310/500) and then Ag (5N purely) was evaporated onto the front side of the Schottky contact at 10^{-6} Torr pressure. This process was repeated for both Cu and Ni (5N purely). Therefore, Ag/*n*-Si/Al, Cu/*n*-Si/Al and Ni/*n*-Si/Al Schottky diodes were fabricated (in Appendix Table 1a, 1b). In addition, the value for each temperature was as follows: T1: 400ºC, T2: 420ºC, T3: 440ºC, T4: 460ºC, T5: 480ºC. For example, T1Ag represents Ag/*n*-Si/Al at 400ºC and T2Cu represents Cu/*n*-Si/Al at 420ºC. T1, T2,… T5 represents D1, D2,… D5, respectively.

2.2. Diode Measurements and Plots

IF (n_{IV}, n_{Ch1}), barrier height (Φ_{IV}, Φ_{CV}, Φ_{Ch2}), built-in potential (V_{bi}), donor concentration (N_D), Fermi level (E_F), interfacial thickness (D_{it}), interface state density (N_{ss}) were calculated from the current-voltage (*I-V*) and capacitance-voltage (C_s-*V*) data [1-5,7-14, 16]. The characteristics of the Schottky diode were calculated from ln(*I*)-*V* measurement and plotted depending on the voltage and the increasing ohmic temperatures. C_s-*V* measurements were performed at room temperature (300^0K) for 250 kHz frequency [7-15]. After the characteristics were obtained, DCD and DDCD were graphed as DCD versus increasing ohmic temperatures (Q_{DCD0}-T_{OT}; where DCD0 is DCD under zero-voltage), DCD versus application plus voltage (Q_{FB}-V_a; where FB is the forward bias) and DCD versus application minus voltage (Q_{RB}-V_a; where RB is the reverse bias).

2.3. Ideality Factor

The IF determines the main feature of a diode. The Schottky diode's current-voltage characteristics have been expressed according to the thermionic emission theory [1, 2, 10, 11, 17-23]. In the case of forward bias for non-ideal condition, the thermionic current equation is as follows:

$$I = \underbrace{AR_n^*T^2 exp\left(-\frac{e\Phi_{BH}}{kT}\right)}_{I_0}\left[exp\left(\frac{e(V-IR_s)}{nkT}\right)-1\right] \tag{1}$$

where *n* is the IF, *V* is voltage, *e* is the electron charge, R_s is the series resistance, *k* is the Boltzmann constant, *T* is the temperature in Kelvin and I_0 is the saturation current. Additionally, R^*_n is the Richardson constant (120 A/cm² K² for *n*-type Si). *A* is the active diode area (using masking radius is 0.4 mm in the experiment), and Φ_{BH} is the effective barrier height.

IF (*n*) has no dimension and is identified from the slope of the linear of the curve in the case of the forward bias and reverse bias. The n_{FB} and n_{RB} were obtained from the following equation [1, 2, 7-15, 18, 19]:

$$n = \frac{e}{kT}\frac{dV}{d(lnI)}. \tag{2}$$

The values of IF were obtained from *I-V*, C_s-*V* and Ch2 functions given in Appendix Table 1a, 1b for the case of forward bias and reverse bias. In the present study, essential characteristic only were given as *I-V* data and in the case of forward bias and DCD was examined with forward bias and reverse bias parameters. Figure 1a shows to the I-V data curves and Figure 1b shows the fits one of them.
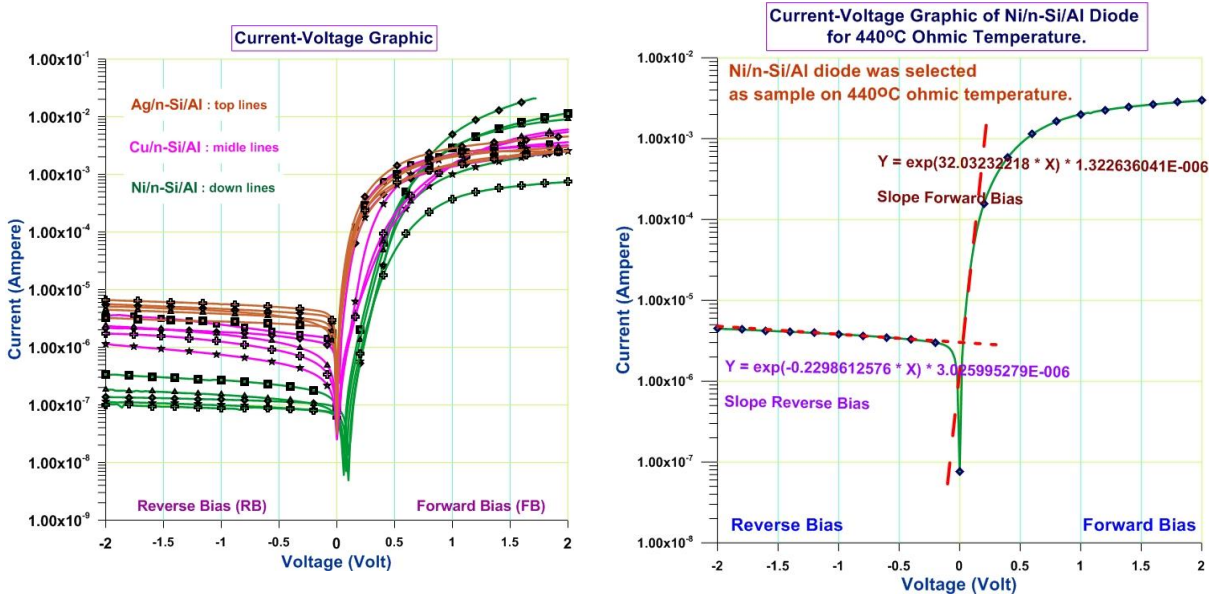

Figure 1. *a) Current versus voltage (lnI-V) graphics (Green lines are Ag/n-Si/Al, magenta lines are Cu/n-Si/Al, brown lines are Ni/n-Si/Al), b) Fits belonging to a diode in the case of forward bias and reverse bias [1-5, 7-16]*

Figure 2a shows IF versus ohmic temperatures. When the figure is examined in detail, it can be seen that IF varies according to the increase in ohmic temperature. It can also be seen that the IF of all diodes increases linearly, except for Ag/*n*-Si at 400ºC and 440ºC. The behaviors of Cu/*n*-Si and Ni/*n*-Si show similarities. Selecting ohmic temperature is a very important process. Diode quality depends on ohmic temperature and ohmic temperature is different for every metal contact which must be followed from the literature [1, 9].
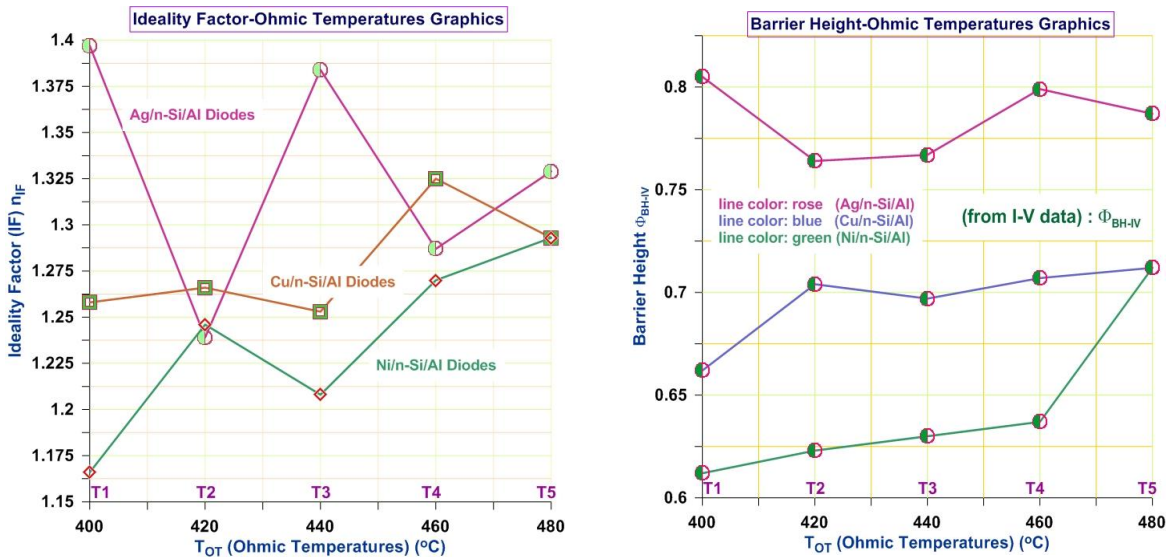

Figure 2. *(a) IF (from I-V) versus ohmic contact temperatures for every diode type, (b) BH (from I-V) versus ohmic contact temperatures and diode type. The symbols represent BH. The color lines show the type of the diodes, and each temperature value is represented as follows: T1: 400ºC, T2: 420ºC, T3: 440ºC, T4: 460ºC, T5: 480ºC. Additionally, there are values of three diodes on every ohmic temperature. T1, T2,... T5 represents D1, D2,... D5, respectively*

2.4. Barrier Height

The barrier height (BH) determines the essential feature of a Schottky diode. The following formula [1-15, 18-24] is used to calculate BH:

$$\Phi_{BH} = \frac{kT}{e} ln \left[\frac{AR^*T^2}{I_0} \right].$$ (3)

The BH was obtained from *I-V*, C_s-*V* and Ch2 functions given in Appendix Table 2a and 2b. Figure 2b shows BH versus ohmic temperatures. When Figure 2b is examined it can be seen that the BH of all of the diodes increased linearly. The behaviors of Ag/*n*-Si and Cu/*n*-Si showed similarities while the Ni/*n*-Si diode firstly increased steadily and then increased abruptly where it was almost linear until 460ºC, the reason being the variation of increasing ohmic temperature in the case of forward bias.

2.5. Cheung Functions

The IF can also be obtained from Ch1 function. Cheung functions are essential in the calculations of IF, BH and serial resistance values. Serial resistance and BH are obtained from the Cheung functions. IF and BH can also be extracted from *I-V* data and compared with each other. The Cheung functions are given as follows [5, 6, 10, 11]:

$$H(I)_{Ch1} = \frac{dV}{d(ln\,I)} = IR_s + \frac{n_{IV}kT}{e} \quad ; \quad H(I)_{Ch2} = IR_s + n_{Ch1}\Phi_{BH}.$$ (4)

The equation on the left is the equation of Paoli and Barns (1976). Indeed, that equation belongs to both scientists is referred by most researchers as Ch1 equation [5, 6]. For convenience, Cheung functions were only shown for the Ag/*n*-Si/Al diode (Figure 3a). The Cheung functions for the other diodes values can be seen in Appendix Table 1a, 1b, 2a, 2b and 4b.
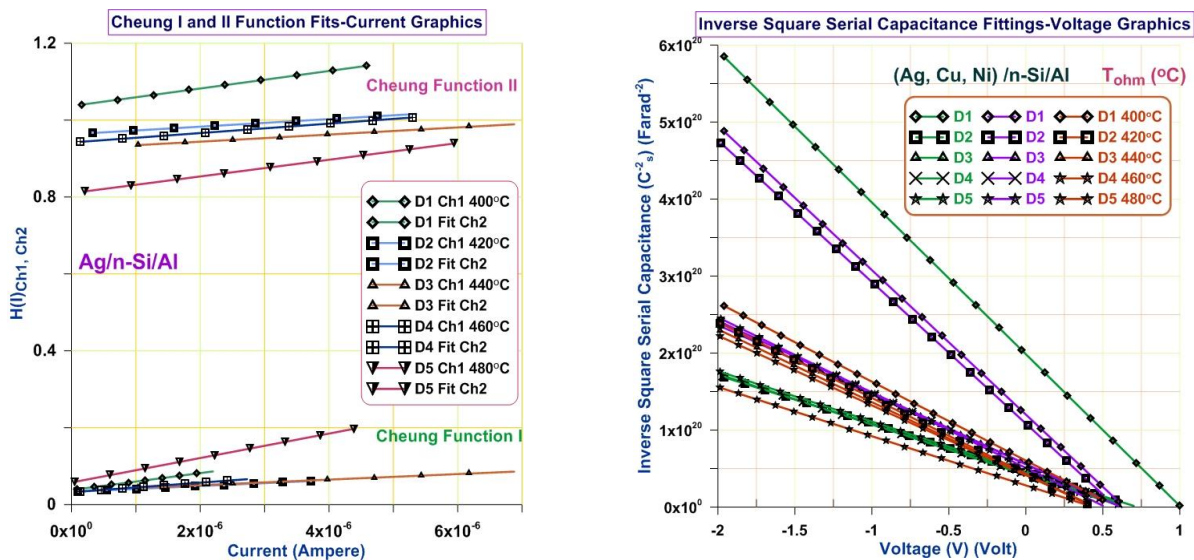

Figure 3. *Ch1 and Ch2 function fittings versus current graphics, (a) for Ag/n-Si diodes, (b) Inverse Square Capacitance-Voltage (C⁻²-V) fits versus voltage graphics (in Appendix Table 1a, 1b, 2a, 2b) (Color lines represent the following: green lines are Ag/n-Si/Al, magenta lines are Cu/n-Si/Al, brown lines are Ni/n-Si/Al. The symbols represent the ohmic temperatures as follows: diamond: T1: 400ºC, square: T2: 420ºC, triangle: T3: 440ºC, star: T4: 460ºC, cross: T5: 480ºC). T1, T2,... T5 represents D1, D2,... D5, respectively*

2.6. C_s-V Graphics

The C_s-V measurements of (Ag, Cu, Ni) metal/n-Si diodes were performed for 250 kHz frequencies at room temperature at dark medium. From the C_s-V measurements, C_s^{-2}-V fitting lines were plotted for (Ag, Cu, Ni)/*n*-Si/Al Schottky diodes and the donor concentration for each metal diode was extracted from their fittings (Figure 3b) (see in Appendix Table 4a). In addition, the built-in potential was obtained from the intercepting points on the V-axis after which DCD could be calculated.

3. DEPLETION CHARGE DENSITY

3.1. Generally Depletion Length

When the vacuum of a vacuum chamber is adjusted, pure metals can be evaporated onto semiconductor surface. Pure metals must be selected regarding the differential work function [1-15] of the metals and the semiconductor. Thermal electrons move from the semiconductor to the metal and leave holes in the semiconductor. Simultaneously, the recombination processes take place and this process is called "contacting" [10, 11, 18, 24]. The electron number on the semiconductor side of the contact decreases and a high resistive zone occurs without charge carriers. The contact formation process continues until the Fermi levels of the semiconductor and metal are balanced. This is known as "Fermi level pinning" [21, 23]. While the positive charged zone occurs in the metal side, the negative charged region takes place in the semiconductor side. A distance without electrical charge is created in between the metal and the semiconductor area. This distance is called a depletion region or space-charge zone [10, 11, 18, 21]. The zone potential field shows up due to the polarized interface. The built-in potential is the reason for zone potential [10, 11, 21-24]. The built-in potential appears as the interface layer. In addition, the built-in potential has to obey the differential work function of the semiconductor and metal and acts as a BH for moving electrical carriers. The built-in potential effective zone is called "depletion layer region" which is perpendicular to the diode surface. The depletion layer distance is also called depletion layer length or depletion length (DL). DL is obtained by the Poisson's equation for a voltage-distance equation, which has a quadratic function [10, 11, 18]. L_0 is the zero-voltage depletion length (ZDL or DL0) in steady state. The built-in potential is never zero while the application potential (V_a) is zero. When the applied voltage is zero or the built-in potential ($V_{bi} \neq 0$) is not zero, formula DL0, L_0 is given as follows [10, 11, 17-24]:

$$L_0 = \sqrt{\frac{2\varepsilon_0\varepsilon_S V_{bi}}{eN_D}} = \sqrt{\frac{2\varepsilon_0\varepsilon_S(\phi_M - \phi_S)}{e^2 N_D}} \tag{5}$$

where L_0 is zero-voltage depletion length and, ε_s is dielectric constant of semiconductor, ε_0 is permeability of the vacuum, V_{bi} is the built-in potential, e is electron's charge unit, ϕ_M is work function of the metal, ϕ_S is affinity of the semiconductor. In the presence of applied voltage, the equations are given as follows in the case of forward bias and reverse bias

$$L_{FB} = \sqrt{\frac{2\varepsilon_0\varepsilon_S\left(V_{bi} - V_a\right)}{eN_D}} \quad , \quad L_{RB} = \sqrt{\frac{2\varepsilon_0\varepsilon_S\left(V_{bi} + V_a\right)}{eN_D}} \tag{6}$$

where V_a is applied voltage [18, 21].

3.2. Obtaining The Depletion Charge Density

The depletion layer region starts from the metal-semiconductor interface and ends at the end of the DL value into a semiconductor. MS contact may be considered as a plate capacitor. As a consequence, capacitor plates have charge density [14, 15, 17, 18].

$$C_{DL} = \frac{dQ_{DL}}{dV} = \frac{d(qN_D L_{DL})}{d[q(N_D/2\varepsilon_0\varepsilon_S)L_{DL}^2]} = \frac{\varepsilon_0\varepsilon_S}{L_{DL}}. \tag{7a}$$

However, charge density does not change linearly between plates in the depletion layer region. DL obeys to the Poisson's equation solution as quadratic equation. The DCD equation may be derived from DL equations by using Equations 5 and 6. Therefore, after the abbreviation of DCD is used in the text, it will not be written again in the formulae as a subindex. For example, Q_{DCD0} is equivalent to Q_0 for simplicity. In the absence of the applied voltage or the presence of built-in potential ($V_{bi} \neq 0$) formula Q_0 is given as follows [18, 19]:

$$Q_0 = \sqrt{2\varepsilon_0\varepsilon_S e N_D V_{bi}}. \tag{7b}$$

In the presence of applied voltage and built-in potential, formulae for forward bias and reverse bias are as follows:

$$Q_{FB} = \sqrt{2\varepsilon_0\varepsilon_S e N_D \left(V_{bi} - V_a\right)} \quad , \quad Q_{RB} = \sqrt{2\varepsilon_0\varepsilon_S e N_D \left(V_{bi} + V_a\right)} \tag{8a}$$

$$Q_{FB} = Q_0 \sqrt{1 - \frac{V_a}{V_{bi}}} \quad , \quad Q_{RB} = Q_0 \sqrt{1 + \frac{V_a}{V_{bi}}}. \tag{8b}$$

Using to the Equation 8a and 8b, voltage range applies from 0 to +4 volts for forward bias and after to from -4 to 0 volts for reverse bias. Q_{FB} and Q_{RB} plot are drawn versus voltage (see Figure 4).
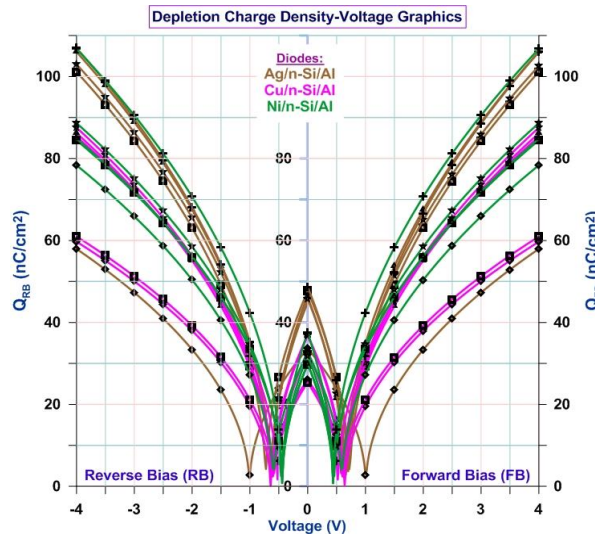

Figure 4. *Depletion charge density-voltage ($Q_{FB/RB}$-V) graphics (Color lines represent the following: green lines are Ag/n-Si/Al, magenta lines are Cu/n-Si/Al, brown lines are Ni/n-Si/Al. Symbols are represented to the ohmic temperatures; diamond: 400°C, square: 420°C, triangle: 440°C, star: 460°C, cross: 480°C and each temperature value represent to diode number as D1: 400°C, D2: 420°C, D3: 440°C, D4: 460°C, D5: 480°C). T1, T2,... T5 represents D1, D2,... D5, respectively*

As seen from Figure 4, the DCD curves related to applied voltage are equal, but there is mirror symmetry present for forward and reverse bias according to origin. In Figure 4, the triangulation (or turning) points appear on the x-axis. That point has a value of built-in potential. The triangulation points were found for DDCD not only the forward bias, but also reverse bias. Unfortunately, Equation 8a does not explain the real state. DL is entreated in [10-11], but it has been seen that DL is neither given as equation nor plotted as graphics by any researcher. To explain that, in both cases (for forward and reverse bias), differential depletion length (DDL) must be considered [10, 11].

DCD formulae are connected to the depletion length formulae and obtained using Equations 6, 7 and 8a

$$Q_{FB} = eN_D L_{FB} \quad , \quad Q_{RB} = eN_D L_{RB} \quad , \quad Q_0 = eN_D L_0 \tag{8c}$$

$$L_{FB} = Q_{FB}/eN_D \quad , \quad L_{RB} = Q_{RB}/eN_D \quad , \quad L_0 = Q_0/eN_D. \tag{8d}$$

3.3. Differential Depletion Charge Density

If Equation 8d is written for the DDL formulae, which are $\varDelta L_{FB}=L_{FB}-L_0$ and $\varDelta L_{RB}=L_{RB}-L_0$ [18, 19, 21, 22], the DDCD equations are obtained for forward and reverse bias respectively as follows:

$$\varDelta Q_{FB} = Q_{FB} - Q_0 \Rightarrow \varDelta Q_{FB} = Q_0 \left[\sqrt{1 - \frac{V_a}{V_{bi}}} - 1 \right] \tag{9a}$$

$$\varDelta Q_{RB} = Q_{RB} + Q_0 \Rightarrow \varDelta Q_{RB} = Q_0 \left[\sqrt{1 + \frac{V_a}{V_{bi}}} + 1 \right]. \tag{9b}$$

DDCD is dependent on the applied voltage, built-in potential and the zero-voltage depletion charge density (DCD0 or ZDCD). When DDCD-voltage graphic (ΔQ_{FB}-V) and $(\Delta Q_{RB}$-$V)$ plots are drawn, it can be seen that DDCD has changed in the case of forward bias and reverse bias (Figure 5). The curves shift downward a little in the case of the reverse bias and shifts even further down in the case of the forward bias compared to reverse bias.

When thermal evaporation is carried out on a semiconductor surface, built-in potential or diffusion potential occurs due to the work function difference between the metal and the semiconductor. It should be noted that built-in potential is the fundamental parameter in Schottky diodes. Both in forward and reverse bias, $\varDelta Q_{FB}$ or $\varDelta Q_{RB}$ has a turning point on the V-axes at a built-in-potential value (Figure 5). When Figure 5 is examined, it can be seen that DDCDRB is up to DDCDFB which is characteristic [10, 11, 14].
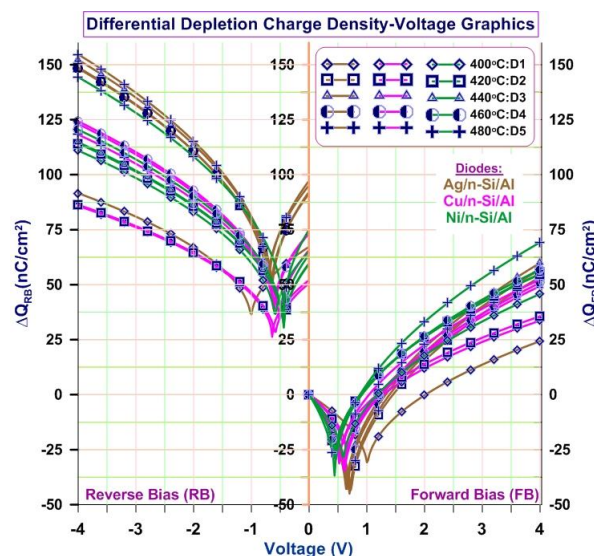
Figure 5. *DDCD-voltage (ΔQ_{FB}-V) graphics and (ΔQ_{RB}-V) graphics (Color lines represent the following: green lines are Ag/n-Si/Al, magenta lines are Cu/n-Si/Al, brown lines are Ni/n-Si/Al. Symbols are represented to the ohmic temperatures; diamond: 400ºC, square: 420ºC, triangle: 440ºC, semimoon: 460ºC, cross: 480ºC and each temperature value represents the following: D1: 400ºC, D2: 420ºC, D3: 440ºC, D4: 460ºC, D5: 480ºC). T1, T2,… T5 represents D1, D2,… D5, respectively*

3.4. Zero-Voltage Depletion Charge Density

ZDCD is determined for a stationary state, while the application potential is zero, the built-in potential is not. ZDCD is a characteristic of ($V_a = 0$; $V_{bi} > 0$). ($V_a = 0$ or $V_{bi} \neq 0$) is a parameter of the original charge density, and therefore comparisons are carried out using this parameter. The said state can easily be seen from Equations 9a and 9b. As seen from Figure 6, ZDCD, for Ag/n-Si, firstly increases sharply, then decreases a little from 420ºC to 460ºC, and then increases again through 480ºC.
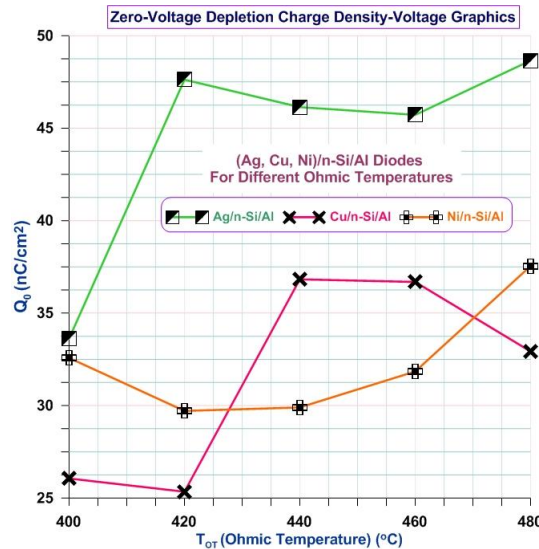

Figure 6. *ZDCD versus ohmic contacted temperatures (Q_0-T_{OT}) ($V_a = 0$ or $V_{bi} > 0$)*

ZDCD, for Cu/n-Si, slowly decreases from 400ºC to 420ºC, increases sharply to 440ºC and stays constant after 440ºC to 460ºC, and decreases at 480ºC. For Ni/n-Si, ZDCD firstly decreases to 420ºC, then slowly increases to 480ºC (see in Appendix Table 5).

3.5. Expansion in a Series of Differential Depletion Charge Density

Equations 9a and 9b are dependent on the applied voltage. Functions are univalent on the built-in potential value (Figures 4 and 5). Both functions take the same value for different applied voltage to 2xV_{bi} in the case of forward and reverse bias. They take the value of an infinite number. Functions are expanded by series to eliminate that problem. If the square root of the DDCD formula is expanded by series, linear equations could be obtained. For both forward bias and reverse bias, the equations are given as follows:

$$\Delta Q_{ExFB} = Q_0 \left(-\frac{V_a}{2V_{bi}} \right) \tag{10}$$

$$\Delta Q_{ExRB} = Q_0 \left(\frac{V_a}{2V_{bi}} + 2 \right). \tag{11}$$

The lines of the Equation 10 and 11 are seen in Figure 7a. Hence, after the abbreviation of Expansion in a Series of Differential Depletion Charge Density (ExDDCD) is used in the text, it will not be written again in the formulae as sub - indexes. For example, the $Q_{DDCDFB/RB}$ is used as a $Q_{FB/RB}$ for simplicity. ExDDCD fitting equations obey to rule of m_1-m_2=0 in analytic geometry. As can be seen from Figure 7b, the intersection point which is shown using a double dotted-line is on the x-axis and the point of the projection shows the voltage. It is equal to two times (2xV_{bi}) to the built-in potential (see Figure 7c and 7d).
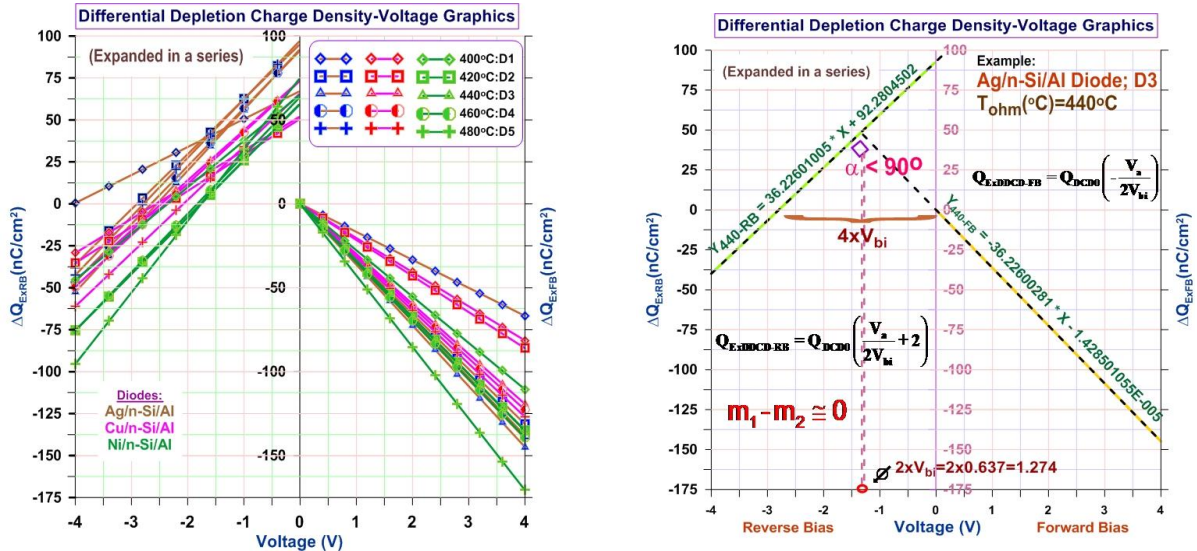
Figure 7. *ExDDCD (Fits)-voltage (ΔQ$_{ExFB/RB}$-V) graphics of Schottky diodes (all in one), (a) lines (left) (b) Ag/n-Si/Al fittings (right) (D3 diode data are chosen randomly)*
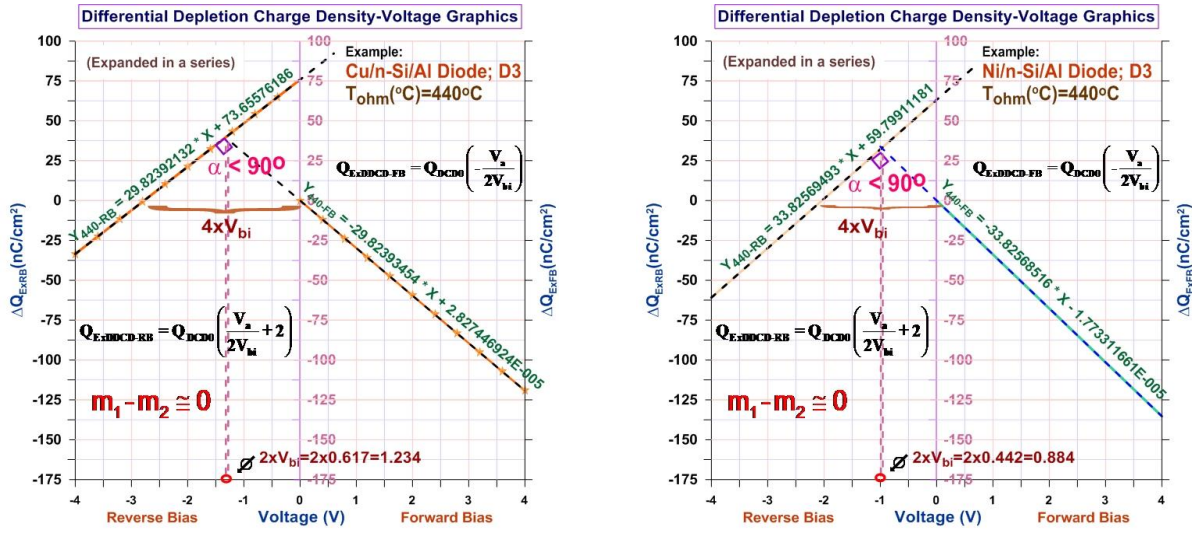
Figure 7. *(c) Cu/n-Si/Al fittings (d) Ni/n-Si/Al fittings (D3 diode data are chosen randomly)*

4. FINDING THE BOUNDARY-VALUES FROM SQUARE ROOTS

We rearrange to Equation 8b, and then it takes to the square and they write as potential rate.

$$\frac{V_a}{V_{bi}} = 1 - \left(\frac{Q_{FB}}{Q_0}\right)^2 \qquad , \qquad \frac{V_a}{V_{bi}} = \left(\frac{Q_{RB}}{Q_0}\right)^2 - 1. \tag{12a}$$

Equation 12a is written in Equation 10 and 11

$$\frac{\Delta Q_{ExRB}}{Q_0} = \frac{1}{2}\left(\frac{Q_{FB}^2 - Q_0^2}{Q_0^2}\right) \quad ; \quad \frac{\Delta Q_{ExRB}}{Q_0} = \left(\frac{1}{2}\left(\frac{Q_{RB}^2 - Q_0^2}{Q_0^2}\right)\right) + 2 \tag{12b}$$

$$\frac{2\Delta Q_{ExFB}}{Q_0} = \frac{(Q_{FB} - Q_0)(Q_{FB} + Q_0)}{Q_0^2} \quad ; \quad \frac{2\Delta Q_{ExRB}}{Q_0} - 4 = \frac{(Q_{RB} - Q_0)(Q_{RB} + Q_0)}{Q_0^2}. \tag{12c}$$

If Equation 12c's left side rearrangement, if Q_{RB} and Q_{FB} write inside into Equation 12c,

$$\frac{2\Delta Q_{ExFB}}{Q_0} = \frac{1}{Q_0^2} Q_0 \left(\sqrt{1-\frac{V_a}{V_{bi}}} - 1 \right) Q_0 \left(\sqrt{1-\frac{V_a}{V_{bi}}} + 1 \right) =$$

$$2\Delta Q_{ExFB} = Q_0 \left[\sqrt{1-\frac{V_a}{V_{bi}}} - 1 \right] \left(\sqrt{1-\frac{V_a}{V_{bi}}} - 1 + 1 + 1 \right) = \Delta Q_{FB} \left(\frac{\Delta Q_{FB}}{Q_0} + 2 \right) \Rightarrow$$

$$\boxed{\Delta Q_{FB}^2 + 2Q_0 \Delta Q_{FB} - 2Q_0 \Delta Q_{ExFB} = 0}. \tag{12d}$$

Thus, a quadratic equation is obtained. If the equation is solved two square roots are found. Equation 12d's final equation handles, and then it regulates

$$\Delta Q_{FB-1,2} = -Q_0 \pm \underbrace{\sqrt{Q_0^2 + 2Q_0 \Delta Q_{ExFB}}}_{=0} \Rightarrow \Delta Q_{FB-1,2} = -Q_0 \tag{12e}$$

two overlapped square roots are obtained.

$$\Delta Q_{FB-1,2} = Q_0 \left[\sqrt{1-\frac{V_a}{V_{bi}}} - 1 \right] = -Q_0 \Rightarrow \sqrt{1-\frac{V_a}{V_{bi}}} = 0 \Rightarrow V_a = V_{bi}. \tag{12f}$$

If DDCD is equal to DCD0, V_a is V_{bi}. Namely, this is true when $V_{net} = V_{bi} - V_a = 0$ in the case of forward bias. The square containing DCD0 terms is as given below

$$Q_0^2 + 2Q_0 \Delta Q_{ExFB} = 0 \Rightarrow \boxed{Q_0 = 0}, \boxed{\Delta Q_{ExFB} = -\frac{Q_0}{2}}. \tag{12g}$$

The $Q_0 = 0$ is not a real state, as it has a real value. If it temporarily assumes a real value, it can be written as a DDCDFB equation

$$\Delta Q_{FB-1,2} = 0 \Rightarrow Q_0 \left[\sqrt{1-\frac{V_a}{V_{bi}}} - 1 \right] = 0 \Rightarrow V_a = 0 \; ; \; V_{bi} \neq 0. \tag{12h}$$

V_a has zero value, which is true when $V_{net} = V_{bi} - 0 = V_{bi}$. Q_0 represents the case in the absence of the applied voltage. Built-in potential is always real in the metal-semiconductor interface even if applied voltage is not. If Equation 12g rewrites in Equation 10, applied potential is equal to built-in potential. That potential is a triangulation potential for Schottky diodes (Figures 4 and 5). The built-in potential is also the boundary-value of the Schottky diode characteristic.

$$\Delta Q_{ExFB} = -\frac{Q_0}{2} \Rightarrow \frac{\Delta Q_{ExFB}}{Q_0} = -\frac{1}{2} \left(\frac{V_a}{V_{bi}} \right) \Rightarrow -\frac{Q_0}{2Q_0} = -\frac{1}{2} \left(\frac{V_a}{V_{bi}} \right) \Rightarrow V_a = V_{bi}. \tag{12i}$$

The same process is repeated for the reverse formulae. If Equation 12c's right side rearranges and if Q_{RB} and Q_{FB} write into inside Equation 12c

$$2\frac{\Delta Q_{ExRB}}{Q_0} - 4 = \frac{(Q_{RB} - Q_0)(Q_{RB} + Q_0)}{Q_0^2} = \frac{1}{Q_0^2} Q_0 \left(\sqrt{1+\frac{V_a}{V_{bi}}} - 1 \right) Q_0 \left(\sqrt{1+\frac{V_a}{V_{bi}}} + 1 \right) \tag{13a}$$

then it is rearranged,

$$2\frac{\Delta Q_{ExRB}}{Q_0} - 4 = \left(\sqrt{1+\frac{V_a}{V_{bi}}}+1-1-1\right)\left(\sqrt{1+\frac{V_a}{V_{bi}}}+1\right) = \left(\frac{\Delta Q_{RB}}{Q_0}-2\right)\frac{\Delta Q_{RB}}{Q_0} \tag{13b}$$

and

$$\boxed{\Delta Q^2_{RB} - 2Q_0\Delta Q_{RB} - 2(Q_0\Delta Q_{ExRB} - 2Q_0^2) = 0} \tag{13c}$$

Thus, a quadratic equation is obtained. When the equation is solved two squares are found. Equation 13c 's final equation handles, and then it regulates

$$\Delta Q_{RB-1,2} = \frac{2Q_0 \pm \sqrt{4Q_0^2 - 4x1x(-2)(Q_0\Delta Q_{ExRB}-2Q_0^2)}}{2}$$

$$\Delta Q_{RB-1,2} = Q_0 \pm \underbrace{\sqrt{2Q_0\Delta Q_{ExRB}-3Q_0^2}}_{=0} \Rightarrow \Delta Q_{RB-1,2} = Q_0. \tag{13d}$$

If DDCDRB is Q_0,

$$\Delta Q_{RB-1,2} = Q_0\left[\sqrt{1-\frac{V_a}{V_{bi}}}-1\right] = Q_0 \Rightarrow \sqrt{1-\frac{V_a}{V_{bi}}} = 2 \Rightarrow V_a = -3V_{bi}. \tag{13e}$$

it is shown that DDCDRB is zero to $V_a=-3V_{bi}$ value.

$$2Q_0Q_{ExRB} - 3Q_0^2 = 0 \Rightarrow Q_0(2\Delta Q_{ExRB}-3Q_0) = 0 \Rightarrow$$

$$Q_0 = 0 \; ; (2Q_{ExRB}-3Q_0) = 0 \Rightarrow \boxed{\Delta Q_{ExRB} = \frac{3}{2}Q_0}. \tag{13f}$$

When the last terms and roots are used, the same results for applied voltage and built-in potential in the case of reverse bias are found, however the results are different for the forward bias. If the Equation 13f rewrites in Equation 11, applied potential is equal to minus built-in potential. This potential is a triangulation potential for Schottky diodes in the case of the reverse bias (Figures 4 and 5).

$$\Delta Q_{ExRB} = \frac{3Q_0}{2} \Rightarrow \frac{\Delta Q_{ExRB}}{Q_0} = \left(\frac{V_a}{2V_{bi}}+2\right) \Rightarrow \frac{3}{2} = \frac{V_a}{2V_{bi}}+2 \Rightarrow V_a = -V_{bi}. \tag{13g}$$

5. CONCLUSION

It has been seen that (Ag, Cu, Ni)/n-Si/Al diode characteristics vary in accordance with the increase in ohmic contact temperature. Schottky parameters can have various fluctuations (Figure 2). Ohmic contact temperature is one of the most important parameters. This study showed the importance of selecting the correct ohmic contact temperature. The literature shows how the temperatures of the Schottky diode parameters change on both sides (namely, Schottky side and Ohmic side properties) [18]. Selecting the ohmic temperature affected the specific resistance of the ohmic side of the Schottky diode. If the correct ohmic temperature is selected, the diode conducts better rectification. In such cases, thermionic-emission regime dominates the current transport [10-15, 18, 24]. Figure 6 reveals the connection between the DCD0 and the ohmic temperature. DCD0 has different value for each temperature value. If DDCD is expanded in a series in the case of the reverse bias and forward bias, DDCD are transformed into the

ExDDCD (it expands in a series because Equation 9a and Equation 9b have got to infinite values, so serial fits yield to mathematical correlation). The ExDDCD has a negative slope for forward bias and a positive slope for reverse bias (Figure 7b, 7c, 7d). The fittings of ExDDCD follow the rule of m_1-$m_2 \approx 0$ for both cases. In Figure 7b, 7c and 7d only the D3 line fitting is shown, but the other lines (i.e. the first, the second, etc.) follow the same rule. However, in Figure 7b, 7c and 7d the slopes are equal after the comma decimal digits, and in y=ax±b equation, ±b may be found slightly different. In this case, y=ax±b equation can be approximated as y≈ax±b. This state is considered characteristic. As seen from Figure 5, the curves show a turning point in a built-in potential (on the V_a or -V_a values), i.e. the function first decreases to the built-in potential value, then increases. In the last section, boundary-values were obtained with the help of various formulae. It is seen that DCD and DDCD curves have gotten triangulation points on the $V_a=V_{bi}$ or $V_a=-V_{bi}$ in both bias. Additionally, $Q_{ExFB}= Q_0/2$, and $Q_{ExRB}= -3Q_0/2$ were found to overlap on the ExDDCD lines. In short, built-in potential has a vital role for Schottky diodes, and affects all other parameters. Built-in potential gives a general view of the essential features, especially about the changing of Q_0, DCD, DDCD, ExDDCD (Figures 5-7). In future studies, if the range for ohmic contact temperature is chosen to be 400, 420, 430,…500°C, better result can be obtained for metal/n-Si/Al diodes. In conclusion, this study may help in the selection of suitable ohmic temperature for MS contact. It could be said final that DCD's and DDCD's formulae can easily differentiate on applied voltage for forward bias and reverse bias. Then differential capacitance's formulae are confirmed by showing [14, 17-19].

ACKNOWLEDGEMENT

CONFLICTS OF INTEREST

No conflict of interest was declared by the authors.

REFERENCES

[1]   Ayyildiz, E., Temirci, C., Bati, B., and Turut, A., "The effect of series resistance on calculation of the interface state density distribution in Schottky diodes", International Journal Electronics, 88(6): 625-633 (2001). doi.org/10.1080/ 00207210110044396

[2]   Turut, A., Ejderha, K., Yildirim, N., Abay, B., "Characteristic diode parameters in thermally annealed Ni/p-InP contacts", Journal of Semiconductors, (37): 4, (2016).

[3]   Alptekin, S., Altindal, S., "A comparative study on current/capacitance: voltage characteristics of Au/n-Si (MS) structures with and without PVP interlayer", Journal of Materials Science: Materials in Electronics, (30): 6491, (2019). doi.org/10.1007/s10854-019-00954-5

[4]   Yeriskin, S.A., Balbasi, M., Orak, I., "The effects of (graphene doped-PVA) interlayer on the determinative electrical parameters of the Au/n-Si (MS) structures at room temperature", Mater Science: Mater Electron, (28):14040, (2017). doi: 10.1007/s10854-017-7255-1

[5]   Cheung, S.K., and Cheung, N.W., "Extraction of Schottky diode parameters from forward current-voltage characteristics", Applied Physics Letter, 49(2): 85-87, (1986).

[6]   Paoli, T.L, and Barnes, P.A, "Saturation of the junction voltage in stripe-geometry (AlGa)As double-heterostructure junction lasers", Applied Physics Letter, (28): 714, (1976).

[7]   Ejderha, K., Zengin, A., Orak, I., Tasyurek, B., Kilinc, T., and Turut, A., "Dependence of characteristic diode parameters on sample temperature in Ni/epitaxy n-Si contacts", Materials Science in Semiconductor Processing, (14): 5–12, (2011).

[8]   Horvath, Z.J., "Evaluation of the interface state energy distribution from Schottky I-V characteristics", Journal Applied Physics, 63(3): 976-978, (1988). doi.org/10.1063/1.340048

[9]   Hudait, M.K., and Kurupanidhi, S.B., "Interface state density distribution in Au/n-GaAs Schottky diodes on n-Ge and n-GaAs substrates", Material Science and Engineering, B(87): 141-147, (2001).

[10]   Korkut, A., "New serial resistance equations: Derivated from Cheungs' functions for the forward and reverse bias I", Microelectronic Engineering, 197 (5): 45-52, (2018).

[11]   Korkut A., "On differential depletion length of Schottky diodes with copper-nickel alloy metal of front contact", Turkish Journal of Physics, (42): 587-599, (2018).

[12]   Twarowski, A.J, and Albrecht, A.C., "Depletion layer studies in organic films: Low frequency capacitance measurements in polycrystalline tetracene", The Journal of Chemical Physics, (70): 2255-2261, (1979). doi.org/10.1063/1.437729

[13]   Kennedy, D.P., Murley, P.C., and Kleinfelder, W., "On the Measurement of Impurity Atom Distributions in Silicon by the Differential Capacitance Technique", IBM Journal of Research and Development, 12(5): 399-409, (1968). doi.org/10.1147/rd.125.0399

[14]   Korkut, A., "Differential Depletion Capacitance Approximation Analysis Under DC Voltage For Air-Exposed Cu/n-Si Schottky Diodes", Surface Review and Letters, (25): 4, 18500, (43-12), (2018). doi: 10.1142/S0218625X18500439

[15]   Cowley, A.M., "Depletion Capacitance and Diffusion Potential of Gallium Phosphide Schottky-Barrier Diodes", Journal Applied Physics, 36(10): 3012-3220, (1966).

[16]   Kern, W., "Handbook of semiconductor wafer cleaning technology: science, technology, and applications", Noyes Publications, Westwood, New Jersey, U.S.A, (1993).

[17]   Farag, A.A.M, Yahia, I.S., Fadel M., "Electrical and photovoltaic characteristics of Al/n-CdS Schottky diode", International Journal of Hydrogen Energy, (34): 4906-4913 (2009).

[18]   Sze, S.M., Physics of Semiconductor Devices, J.Wiley-Sons, Singapore, (1981).

[19]   Grundmann, M., "The Physics of Semiconductors", Springer-Verlag Inc, Germany, (2006).

[20]   Rhoderick, E.H., "Metal-semiconductor contacts", IEE Proceedings I-Solid-State and Electron Devices, IEEPROC, 129(1):1, (1982). doi: 10.1049/ip-i-1.1982.0001

[21]   Sharma, B.L., "Metal-Semiconductor Schottky Barrier Junctions and Their Applications", Plenum Press, UK, (1984).

[22]   Böer, K.W., "Introduction to Space Charge Effects in Semiconductors", Springer Verlag Inc, Berlin, Germany, (2010).

[23]   Schroder, D.K., "Semiconductor Material and Device Characterization", J.Willey-Sons, USA, (2006).

[24]   Rhoderick, E.H., and Williams, R.H., "Metal-Semiconductor Contacts", Oxford, Clarendon Press, UK, (1988).

APPENDIX

Table 1a. *Ideality factor values of (Ag, Cu, Ni)/n-Si/Al Schottky diodes (in the case of forward bias)*

°C	Ideality Factor					
Ohmic Temp.	$n_{I\text{-}V}$ Ag/n-Si/Al	$n_{I\text{-}V}$ Cu/n-Si/Al	$n_{I\text{-}V}$ Ni/n-Si/Al	n_{Ch1} Ag/n-Si/Al	n_{Ch1} Cu/n-Si/Al	n_{Ch1} Ni/n-Si/Al
400	1.397	1.253	1.166	1.455	1.299	1.196
420	1.239	1.266	1.246	1.274	1.242	1.209
440	1.384	1.252	1.208	1.242	1.323	1.221
460	1.287	1.325	1.270	1.264	1.232	1.257
480	1.329	1.293	1.293	1.300	1.196	1.320

Table 1b. *Ideality factor values of (Ag, Cu, Ni)/n-Si/Al Schottky diodes (in the case of reverse bias)*

°C	Ideality Factor					
Ohmic Temp.	$n_{I\text{-}V}$ Ag/n-Si/Al	$n_{I\text{-}V}$ Cu/n-Si/Al	$n_{I\text{-}V}$ Ni/n-Si/Al	n_{Ch1} Ag/n-Si/Al	n_{Ch1} Cu/n-Si/Al	n_{Ch1} Ni/n-Si/Al
400	175.2	62.2	162.7	194.9	61.6	164.9
420	111.1	62.4	234.2	110.7	62.2	234.1
440	114.2	70.3	168.3	114.6	70.7	166.9
460	196.3	59.0	103.5	186.4	57.8	102.1
480	391.5	61.8	165.8	394.5	62.2	167.7

Table 2a. *Barrier height values of (Ag, Cu, Ni) /n-Si/Al Schottky diodes (in the case of forward bias)*

°C	Barrier Height (eV)								
Ohmic Temp.	$\Phi_{I\text{-}V}$ Ag/n-Si/Al	$\Phi_{I\text{-}V}$ Cu/n-Si/Al	$\Phi_{I\text{-}V}$ Ni/n-Si/Al	Φ_{Ch2} Ag/n-Si/Al	Φ_{Ch2} Cu/n-Si/Al	Φ_{Ch2} Ni/n-Si/Al	$\Phi_{C\text{-}V}$ Ag/n-Si/Al	$\Phi_{C\text{-}V}$ Cu/n-Si/Al	$\Phi_{C\text{-}V}$ Ni/n-Si/Al
400	0.805	0.663	0.612	0.712	0.509	0.487	1.233	1.031	1.034
420	0.764	0.704	0.623	0.758	0.713	0.508	1.132	0.988	0.885
440	0.767	0.697	0.630	0.674	0.700	0.619	1.011	1.041	0.898
460	0.799	0.707	0.637	0.758	0.734	0.636	1.062	1.001	0.895
480	0.787	0.712	0.712	0.824	0.536	0.458	1.074	0.948	0.891

Table 2b. *Barrier height values of (Ag, Cu, Ni) /n-Si/Al Schottky diodes (in the case of reverse bias)*

°C	Barrier Height (eV)								
Ohmic Temp.	$\Phi_{I\text{-}V}$ Ag/n-Si/Al	$\Phi_{I\text{-}V}$ Cu/n-Si/Al	$\Phi_{I\text{-}V}$ Ni/n-Si/Al	Φ_{Ch2} Ag/n-Si/Al	Φ_{Ch2} Cu/n-Si/Al	Φ_{Ch2} Ni/n-Si/Al	$\Phi_{C\text{-}V}$ Ag/n-Si/Al	$\Phi_{C\text{-}V}$ Cu/n-Si/Al	$\Phi_{C\text{-}V}$ Ni/n-Si/Al
400	0.696	0.653	0.603	0.655	0.680	0.633	0.531	0.522	0.536
420	0.680	0.671	0.615	0.733	0.698	0.635	0.540	0.461	0.540
440	0.695	0.638	0.608	0.706	0.659	0.647	0.539	0.475	0.537
460	0.702	0.662	0.609	0.776	0.699	0.650	0.544	0.477	0.533
480	0.702	0.647	0.598	0.725	0.668	0.624	0.552	0.474	0.541

Table 3. *Built-in potential values of (Ag, Cu, Ni)/n-Si/Al Schottky diodes*

°C	Built-in Potential (V) V_{bi}		
Ohmic Temp.	Ag/n-Si/Al	Cu/n-Si/Al	Ni/n-Si/Al
400	1.007	0.640	0.589
420	0.726	0.589	0.440
440	0.637	0.617	0.442
460	0.663	0.597	0.457
480	0.696	0.519	0.440

Table 4a. *Donor concentration values of (Ag, Cu, Ni)/n-Si/Al Schottky diodes*

°C	Donor Concentration (cm^{-3}) N_D (Forward Bias)			Donor Concentration (cm^{-3}) N_D (Reverse Bias)		
Ohmic Temp.	Ag/*n*-Si/Al	Cu/*n*-Si/Al	Ni/*n*-Si/Al	Ag/*n*-Si/Al	Cu/*n*-Si/Al	Ni/*n*-Si/Al
400	3.324E15	3.143E15	5.334E15	4.168E17	1.553E17	7.447E17
420	9.257E15	3.228E15	5.939E15	8.299E17	1.591E17	1.116E18
440	9.902E15	6.506E15	5.991E15	8.172E17	3.647E17	8.349E17
460	9.343E15	6.672E15	6.569E15	1.425E18	2.970E17	5.353E17
480	1.007E16	6.193E15	9.485E15	2.968E18	2.963E17	1.217E18

Table 4b. *Serial resistance values of (Ag, Cu, Ni)/n-Si/Al Schottky diodes*

°C	Serial Resistance (Ω) R_S (Forward Bias)			Serial Resistance (Ω) R_S (Reverse Bias)		
Ohmic Temp.	Ag/*n*-Si/Al	Cu/*n*-Si/Al	Ni/*n*-Si/Al	Ag/*n*-Si/Al	Cu/*n*-Si/Al	Ni/*n*-Si/Al
400	22023.82	00136.85	327.73	6.528E7	3.585E6	2.314E6
420	07531.43	02168.02	423.48	2.210E7	7.656E6	2.314E6
440	07222.96	10599.36	268.61	2.262E7	2.436E6	2.166E6
460	12315.75	00261.99	459.84	1.044E8	4.815E6	1.375E6
480	09099.49	01883.66	666.12	1.640E8	3.087E6	1.453E6

Table 5. *ZDCD values of (Ag, Cu, Ni)/n-Si/Al Schottky diodes*

°C	ZDCD or DCD0 (Zero-voltage Depletion Charge Density) (nC/cm^2) Q_0					
	(Forward Bias)			(Reverse Bias)		
Ohmic Temp.	Ag/*n*-Si/Al	Cu/*n*-Si/Al	Ni/*n*-Si/Al	Ag/*n*-Si/Al	Cu/*n*-Si/Al	Ni/*n*-Si/Al
400	33.620	26.059	32.578	376.492	183.190	384.945
420	47.622	25.341	29.711	450.893	177.917	407.299
440	46.140	36.828	29.900	419.183	275.726	352.960
460	45.719	36.685	31.844	564.645	244.773	287.460
480	48.657	32.931	37.545	835.149	227.790	425.209